



## Removal of hazardous azo dye Metanil Yellow from aqueous solution by cross-linked magnetic biosorbent; equilibrium and kinetic studies

Servet Tural<sup>a,\*</sup>, Tuba Tarhan<sup>a,b</sup>, Bilsen Tural<sup>a</sup>

<sup>a</sup>Faculty of Education, Department of Chemistry, Dicle University, Diyarbakir 21280, Turkey, Tel. +90 412 2488030/8915; Fax: +90 412 2488257; email: [servet.tural@hotmail.com](mailto:servet.tural@hotmail.com) (S. Tural), Tel. +90 482 2134002; Fax: +90 482 2134004; email: [ttarhan21@gmail.com](mailto:ttarhan21@gmail.com) (T. Tarhan), Tel. +90 412 2488030/8916; Fax: +90 412 2488257; email: [bilsentural@gmail.com](mailto:bilsentural@gmail.com) (B. Tural)

<sup>b</sup>Vocational High School of Health Services, Mardin Artuklu University, Mardin 47100, Turkey

Received 25 February 2015; Accepted 26 May 2015

### ABSTRACT

In this study, glutaraldehyde cross-linked magnetic chitosan nanoparticles (GMCNs) were prepared through cross-linking modification of magnetic chitosan nanoparticles using glutaraldehyde as a cross-linker that exhibited excellent Metanil Yellow (MY) adsorption performance. The characterization of the GMCNs was performed by Fourier transform infrared spectroscopy, transmission electron microscopy, scanning electron microscopy, dynamic light scattering, and vibrating sample magnetometry analyses. Adsorption characteristics of MY from aqueous solution onto GMCNs have been studied. During the studies, various essential factors influencing the adsorption, like adsorbate concentration, amount of adsorbent, pH of the solution, and contact time have been monitored. The equilibrium was achieved within 17 h at pH 4, and the adsorption data obeyed the Langmuir equation with a maximum adsorption capacity of 625 mg/g and a Langmuir adsorption equilibrium constant of  $5.2 \times 10^{-4} \text{ dm}^3/\text{mg}$  at 25°C. The adsorption kinetics of MY at different initial dye concentrations was evaluated by the first-order and second-order models. The kinetic studies of MY adsorption showed that the adsorption process followed a second-order kinetic model. Furthermore, the GMCNs can be regenerated and reused through dye desorption in alkaline solution at pH 10. Adsorption results for reusability were 100, 93, and 65%, respectively, for three repeats.

*Keywords:* Adsorption; Cross-linked-magnetic chitosan; Metanil Yellow; Regeneration; Adsorption isotherm; Adsorption kinetics

### 1. Introduction

Metanil Yellow (MY) is a highly water-soluble azo dye. It is widely used for the coloring of soap, spirit lacquer, shoe polish, bloom sheep dip for the preparation of wood stains, dyeing of leather, manufacture of

pigment lakes, colored water-fast inks, and for staining paper [1–3]. Although the use of MY as a colorant agent is not permitted, it is still widely used as a colorant in many food industries. Therefore, it is often released in effluents during processing and transforming and causing a lot of health and environmental problems [1–3]. Hence, it is a major pollutant and

\*Corresponding author.

various workers have made attempts to remove MY from wastewater [1–4].

A number of chemical and physical methods such as chemical coagulation, activated sludge, biodegradation, oxidation, membrane separation, adsorption, and photodegradation have been reported for the removal of azo dye compounds [5–10]. Among the physical and chemical processes, the adsorption procedure is effective in producing high-quality effluent without the formation of harmful substances [9,10]. A number of adsorption materials have been used to remove dyes and organic compounds including ion exchange resins, hen feather, eggshell, bottom ash, and *Hibiscus cannabinus* fiber [11–16].

In recent years, there has been increased interest in the use of magnetic-assisted separation technique (MAT) which is an alternative to centrifugation or filtration separation methods based on the use of magnetic nanoparticles (MNPs) [17,18]. In the MAT, functionalized MNPs are dispersed into the samples containing target compounds, and then the adsorption of the compounds on the surface of functionalized particles takes place, and subsequently, the magnetic particles containing the adsorbed compounds are collected rapidly and conveniently with an external magnetic field for separation. The removal of these magnetic particles from the solution with the use of magnetic field is more selective and efficient than centrifugation or filtration processes [17,18].

Chitosan is a product of deacetylation process of chitin which is the most popular natural polymer that has increasingly been applied in medicine, pharmacology, biotechnology, as well as plant or environment protection [19,20]. Owing to the fact that it possesses amine and hydroxyl functional groups, it is characterized by a high adsorptive effectiveness of metal ions [21] and dyes from aqueous solutions [10,19–21]. A drawback of chitosan is its solubility in acidic solutions. At  $\text{pH} < 5.5$ , it dissolves and loses its adsorption capacity for sorbate binding. Cross-linking can be considered as a solution to this problem. The cross-linked chitosan maintains constant reactivity in a wide pH range and is characterized by high mechanical resistance [22]. The cross-linking may also affect the improvement of its regeneration properties [23,24].

The aims of this study are to prepare glutaraldehyde cross-linked magnetic chitosan nanoparticles (GMCNs) and to investigate the adsorption characteristics of MY from aqueous solutions onto GMCNs. Furthermore, the influence factors of the adsorption such as pH, contact time, and dye concentrations were studied; the equilibrium isotherm parameters and regeneration were determined and discussed. To the best of our knowledge, there were no reports of

the adsorption characteristics of MY from aqueous solutions onto GMCNs.

## 2. Material and methods

### 2.1. Chemicals and reagents

Iron(III) chloride hexahydrate ( $\text{FeCl}_3 \cdot 6\text{H}_2\text{O}$ ), iron(II) chloride tetrahydrate ( $\text{FeCl}_2 \cdot 4\text{H}_2\text{O}$ ), glutaraldehyde solution (25 wt% in  $\text{H}_2\text{O}$ ,  $\text{C}_5\text{H}_8\text{O}_2$ ), chitosan poly (D-glucosamine) deacetylated chitin, (low molecular weight), sodium acetate trihydrate ( $\text{C}_2\text{H}_3\text{NaO}_2 \cdot 3\text{H}_2\text{O}$ ), mineral oil, Tween 80, and acetone ( $\text{C}_3\text{H}_6\text{O}$ ) were purchased from Sigma–Aldrich. MY ( $\text{C}_{18}\text{H}_{14}\text{N}_3\text{NaO}_3\text{S}$ ) was obtained from Fluka. All reagents were of analytical grade and used without further purification. Deionized water was used throughout the experiments.

### 2.2. Preparation of cross-linked magnetic chitosan nanoparticles

MNPs were prepared by co-precipitation method as reported in our previous work [25,26]. One gram  $\text{Fe}_3\text{O}_4$  nanoparticles were washed with ethanol and dispersed in a solution with 165-mL mineral oil and 2-mL tween-80; then, 10-g chitosan was completely dissolved by stirring in a solution of  $1.0 \text{ dm}^3$ , 1.5 wt% acetic acid. Seventy-five milliliters chitosan solution was dropped into a dispersed solution. The chemical cross-linking reagent glutaraldehyde (15 mL, 25 v/v%) was mixed and shaken for 4 h at 1,500 rpm within the incubator. The adsorbent (GMCNs) was gained after the reaction mixture was separated with a magnet and washed several times with acetone, and finally dried in a freeze dryer.

### 2.3. Characterization of the adsorbent

The particles were analyzed by transmission electron microscopy (TEM) (JEOL 2100 F, Japan) for particle size and morphology. Quanta 400F Field Emission Scanning Electron Microscopy (FE-SEM (FEI)) was used for morphological characterization of GMCNs and MY-adsorbed GMCNs. Fourier transform infrared (FT-IR) spectra was measured on a Thermo Scientific Nicolet IS10FT-IR spectrometer (USA). Sixteen scans were collected at a resolution of  $4 \text{ cm}^{-1}$ . The particle size and distributions of the MNPs and GMCNs were determined using dynamic light scattering (DLS) technique (Zeta Sizer Nano-ZS, Malvern). Magnetization measurements as a function of magnetic field were carried out using a vibrating sample magnetometer (VSM) (Q-3398, Cryogenic).

#### 2.4. Batch studies

The experiments were conducted with 25-mg GMCNs and 10-mL initial dye concentration within the range of 0.4–7.4 mM at pH 4 using 0.1-M acetate buffer solution, then incubated about 24 h with constant shaking at 200 rpm and at 25°C. The aqueous phase was separated from GMCNs by Nd–Fe–B permanent magnet. The dye concentration remaining in the solution was determined at 434 nm using a UV/visible spectrometer (Perkin Elmer Lambda 25) after the pH was adjusted to 6 using either hydrochloric acid or sodium hydroxide standardized solutions since the

$\lambda_{\max}$  of dye solution can be varied at different pH [27,28]. The preparation steps of GMCNs and using for the adsorption of MY dye are shown in Fig. 1.

The effect of MY adsorption was studied in the pH range 3–8. The pH of the initial solution was adjusted to the required pH value using either HCl or NaOH solution. All experiments were conducted in triplicate and the mean values have been reported.

#### 2.5. Regeneration and reusability of the adsorbent

Regeneration of the adsorbent was studied by placing 150-mg GMCNs into 10-mL dye solutions

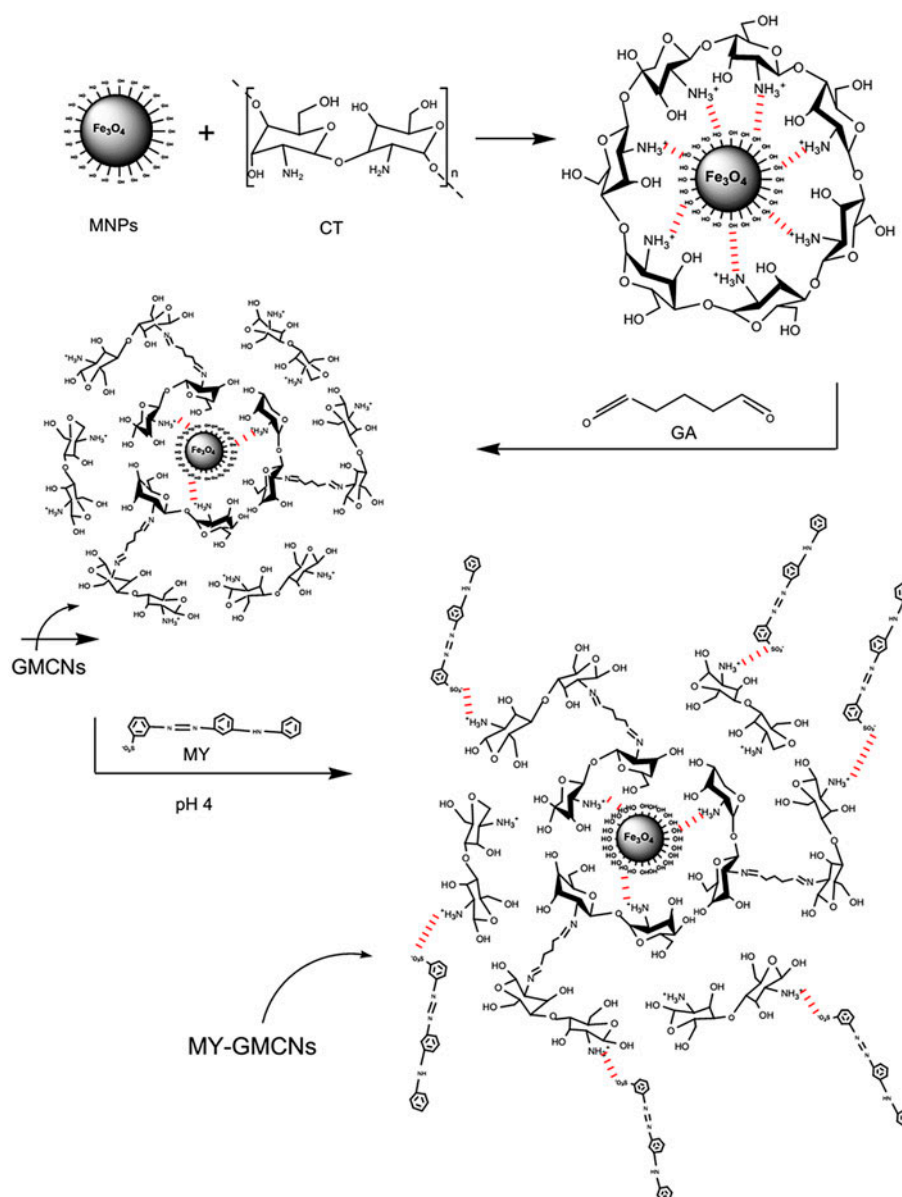


Fig. 1. Schematic illustration for the preparation steps of glutaraldehyde (GA) cross-linked magnetic chitosan nanoparticles (GMCNs) and using for MY adsorption.

(7.4 mM, pH 4.0) with constant shaking at 150 rpm and 25°C for 120 min. Dye-loaded GMCNs were collected and removed from the solution by a magnet, and then the dye-loaded GMCNs were agitated with 10-mL  $\text{NH}_4\text{OH}/\text{NH}_4\text{Cl}$  buffer at pH 10.0 for 120 min at 25°C. The reusability of the adsorbents was studied by reusing the desorbed GMCNs in adsorption experiments. The process of experiments was repeated three times.

### 3. Results and discussions

#### 3.1. Characterization of the GMCNs

The magnetic properties of MNPs and GMCNs were investigated by VSM analysis at room temperature. The saturation magnetization of MNPs (see Fig. 2(A)) and GMCNs (see Fig. 2(B)) were about 66.0 and 22.0  $\text{emu g}^{-1}$ , respectively. The decrease in the saturation magnetization of nanoparticles after coating can be explained by the decrease in the amount of the magnetic moments per unit weight due to the diamagnetic contribution of chitosan shell [29]. The solid phase was separated from the mixture by magnetic separation with the help of a permanent magnet. As can be seen in Fig. 2(C), the GMCNs were highly responsive to a magnetic field, where the slurry was clarified in 30 s using a permanent magnet.

The particle agglomeration size distributions of the MNPs and GMCNs were shown in Fig. 3(A) and (B).

These results suggest that the particle agglomeration size of the MNPs increased significantly from 126 to 762 nm when they were coated with glutaraldehyde cross-linked chitosan. As can be seen from the TEM image in Fig. 3(C), for the GMCNs, the number length (arithmetic) mean size of the primary particles is approximately 11 nm. The observation of surface morphology of the unloaded and MY-loaded GMCNs is shown in Fig. 3(D) and (E). As can be seen from the SEM image, the surface is rough, non-porous, folded, and non-hollow.

The FT-IR spectra of pure chitosan, GMCNs, and MY-adsorbed GMCNs are shown in Fig. 4. The spectrum of chitosan displays a number of absorption peaks, an indication of different types of functional groups present in chitosan beads. The broad and strong band ranging from 3,200 to 3,600  $\text{cm}^{-1}$  corresponds to the presence of  $-\text{OH}$  and  $-\text{NH}_2$  groups, which are consistent with the peak at 1,024 and 1,650  $\text{cm}^{-1}$  assigned to alcoholic C–O stretching vibration and the characteristic of amine (N–H) deformation. After chitosan was coated on MNPs, O–H and C–H stretching vibration and  $-\text{NH}_2$  deformation peaks of chitosan appear at 3,287, 2,867, and 1,650  $\text{cm}^{-1}$  [29], respectively, in the spectra of GMCNs. The existence of these characteristic peaks of chitosan indicates that chitosan was coated onto MNPs. After the adsorption of MY onto GMCNs, the characteristic peaks of S=O and N=N groups are observed at 1,139 and 1,584  $\text{cm}^{-1}$ , respectively. Presence of these peaks in the FT-IR

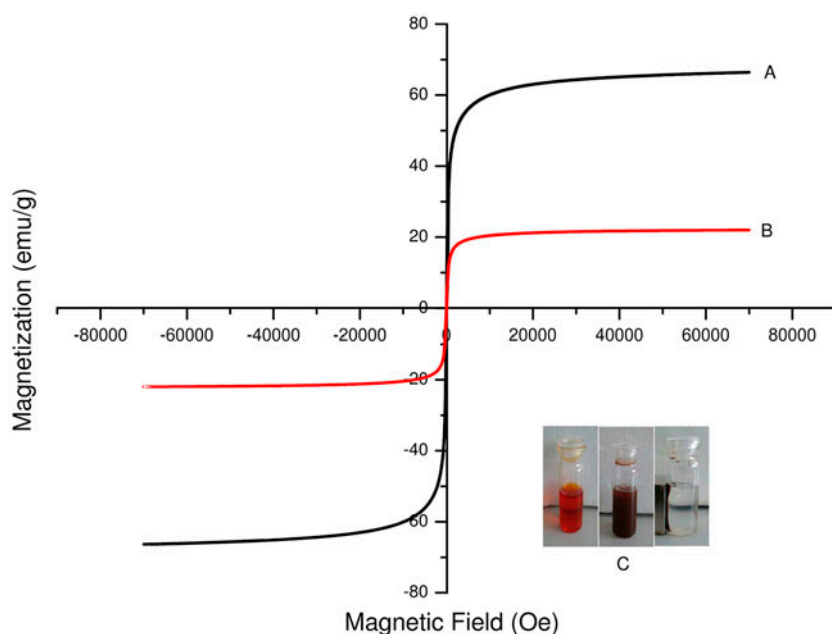


Fig. 2. Magnetization vs. magnetic field for nanoparticles. (A) MNPs, (B) GMCNs, and (C) response of the cross-linked magnetic chitosan nanoparticles to the magnetic field.

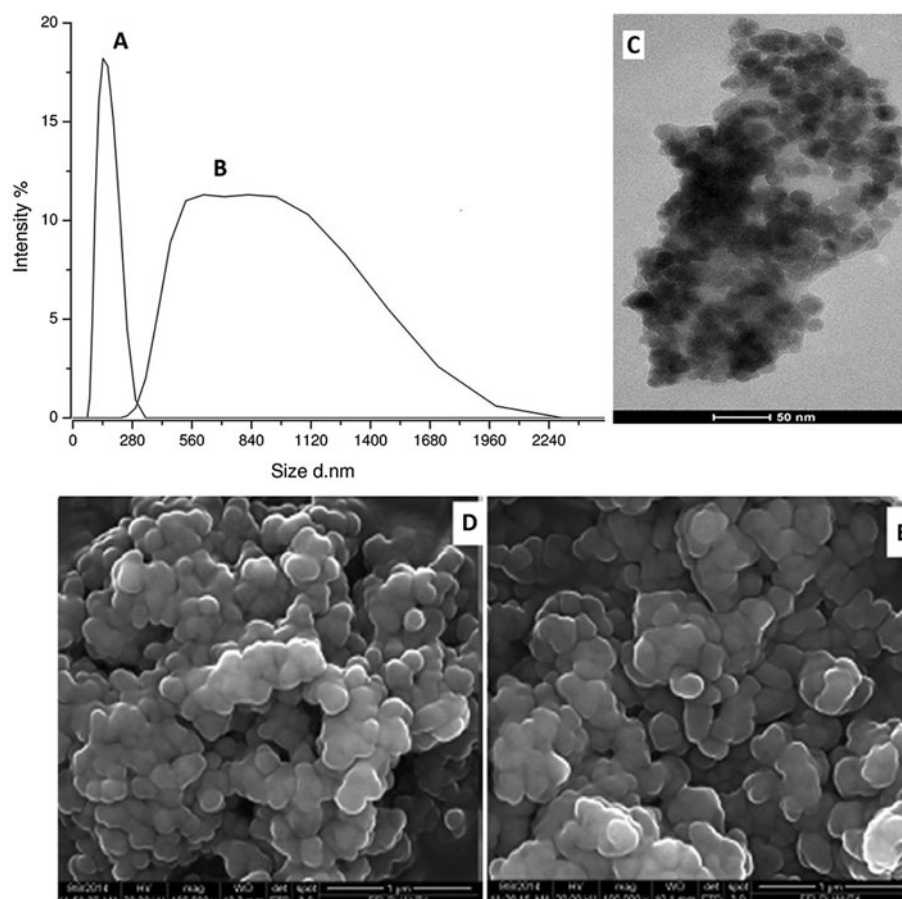


Fig. 3. (A) Particle agglomeration size distribution of the naked Fe<sub>3</sub>O<sub>4</sub>, (B) particle agglomeration size distribution of GMCNs, (C) TEM for GMCNs, the bar is 50 nm, (D) SEM for GMCNs, and (E) SEM for MY-adsorbed GMCNs, the bars are 1 μm for each sample.

spectrum of GMCNs indicates that MY molecules were adsorbed onto the GMCNs.

### 3.2. Investigation of sorption parameters

In order to optimize the pH for maximum removal efficiency, experiments were conducted in the pH range from 3.0 to 8.0 using 50-mg GMCNs with 50-mL of 2.5-mM adsorbate solutions at room temperature (see Fig. 5). The experimental adsorption capacities of MY increased from 208- to 221-mg/g adsorbent as the initial pH of the solution decreased from 8.0 to 3.0. The protonation of amino groups of chitosan is much easier in the acidic solution. Thus, increasing the electrostatic attraction between  $-\text{SO}_3^-$  of the dye and  $-\text{NH}_3^+$  of chitosan causes an increase in the dye adsorption process [30,31]. The results indicated that the removal of dye increased between pH 3 and 4 then decreased with pH variation from 4 to 8.

The effect of agitation time on the extent of adsorption of MY at different concentrations is shown in Fig. 6. The extent of adsorption increases with time and attains equilibrium for all the concentrations of MY studied (2.5, 3.8, and 5.6 mM) at 17 h. After this equilibrium period, the amount of MY adsorbed did not change significantly with time, indicating that this time is sufficient to attain equilibrium for the maximum removal of MY from aqueous solutions by GMCNs.

The adsorption data of MY concentration vs. percent dye removal and amount of dye adsorbed ( $q_e$ ), by GMCNs (see Fig. 7(A)) indicated that as the initial concentrations of MY increased from 0.5 to 2.5 mM, the percent dye removal remained approximately stable. However, the percent dye removal after 2.5 mM decreased from 99 to 48%, as the initial MY concentration increased from 2.5 to 7.6 mM (see Fig. 7(A)).

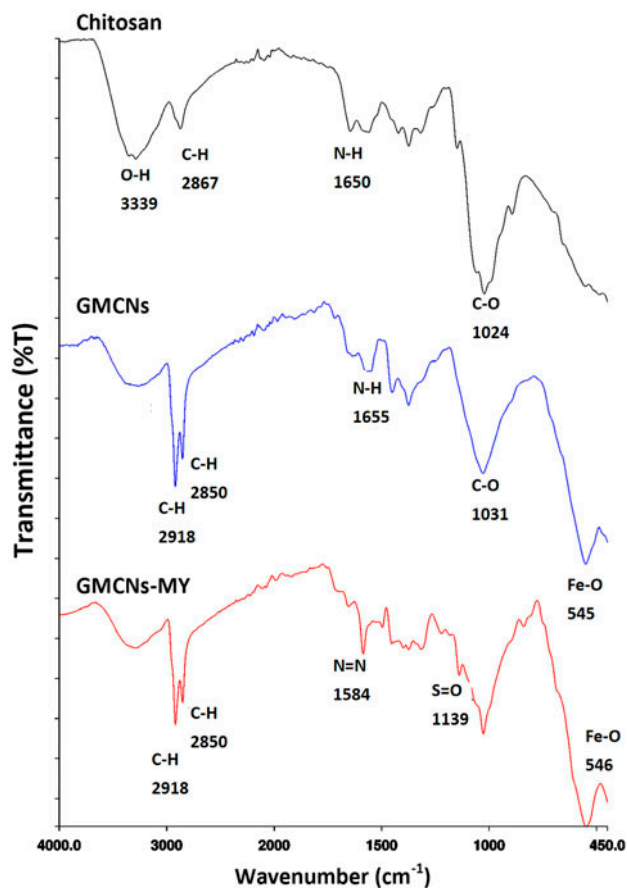


Fig. 4. FT-IR spectra of samples for chitosan, GMCNs, and MY-adsorbed GMCNs.

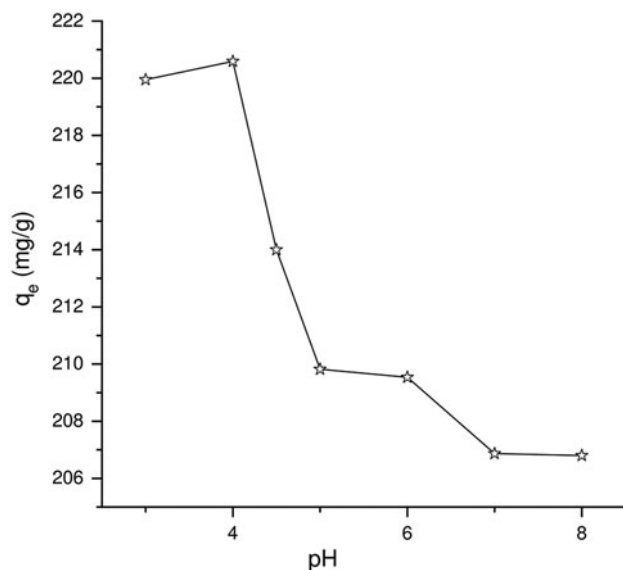


Fig. 5. The effect of pH for adsorption capacities of MY onto GMCNs as 2.5-mM initial dye concentration and 50-mg GMCNs.

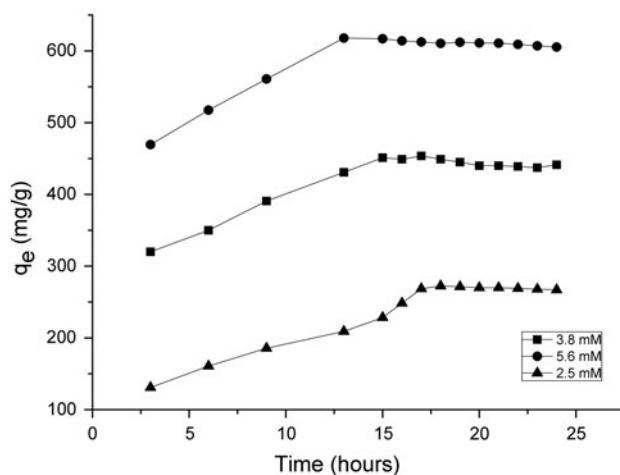


Fig. 6. The kinetics of the adsorption capacity of MY for different initial concentrations onto GMCNs.

The effect of the adsorbent dose on the biosorption of MY was conducted at an initial MY concentration of 5.6 mM and 200 rpm stirring rate for 17 h at 25°C. As can be seen in Fig. 7(B), the percentage removal of MY increases with increase in the adsorbent doses, while the sorption capacity,  $q_e$  (mg/g), at equilibrium decreases. This can be attributed to the increased adsorbent surface area and availability of more sorption sites on the adsorbent. The results clearly indicated that the removal efficiency increases up to an optimum dose of 70 mg and thereafter the percent removal of MY remained to be constant. The maximum percent removal of MY is about 99% with 70-mg GMCNs.

### 3.3. Adsorption isotherm models

Distribution of MY between the liquid phase and the solid phase can be described by Langmuir and Freundlich isotherm models. The Langmuir model assumes that the adsorption of the dye occurs on a homogenous surface by monolayer adsorption with no transmigration of the dye in the plane surface [32,33]. The Langmuir equation may be written as (1, 2):

$$\frac{C_e}{q_e} = \frac{1}{K_L q_m} + \frac{C_e}{q_m} \quad (1)$$

$$q_m = \frac{K_L}{b} \quad (2)$$

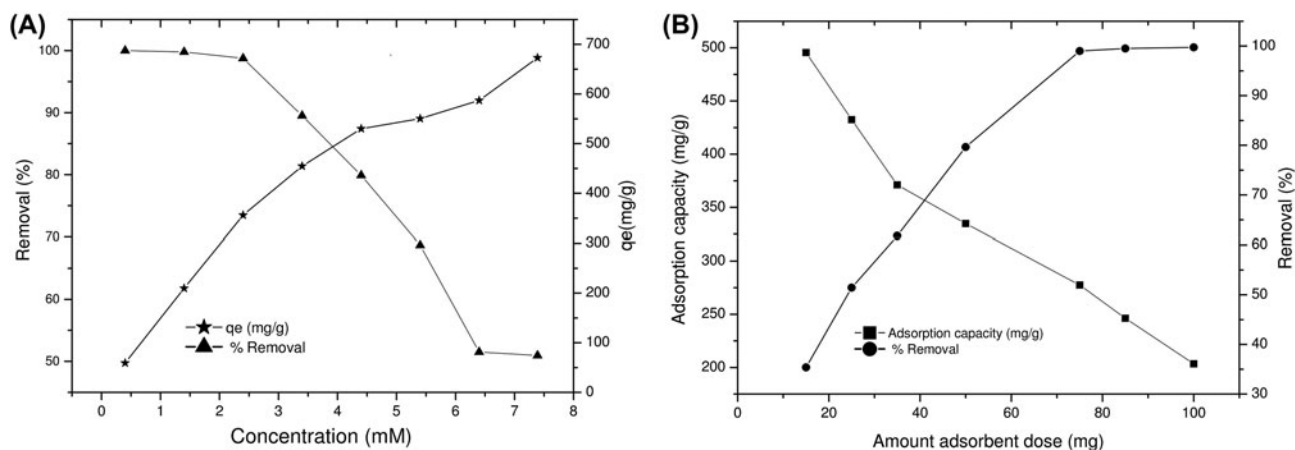


Fig. 7. Effect of (A) concentration and (B) adsorbent dose on the removal of MY.

Table 1

Langmuir and Freundlich isotherm parameters for adsorption of MY onto GMCNs

Langmuir constants				Freundlich constants		
$K_L$ (dm <sup>3</sup> /g)	$b$ (dm <sup>3</sup> /mg)	$q_m$ (mg/g)	$R^2$	$K_F$ (dm <sup>3</sup> /g)	$n$	$R^2$
0.032	$5.2 \times 10^{-4}$	625	0.99	143.1	4.47	0.88

where  $q_e$  is amount of dye adsorbed (mg/g),  $C_e$  is equilibrium concentration of MY in solution (mg L<sup>-1</sup>), and  $q_m$  is maximum monolayer adsorption capacity of dye onto 1-g adsorbent (mg/g). The constant  $b$  (L mg<sup>-1</sup>) in the Langmuir equation is related to the energy or the net enthalpy of the sorption process. The constant  $K_L$  (L g<sup>-1</sup>) can be used to determine the enthalpy of adsorption [34]. The constants  $b$  and  $K_L$  are the characteristics of the Langmuir equation and can be determined from the linearized form of the Langmuir equation (2) [34]. A linearized plot of  $C_e/q_e$  against  $C_e$  gives  $K_L$ ,  $q_m$ , and  $b$ . The Langmuir isotherm constants and  $q_m$  are given for anionic dye MY at pH 4 and at 25°C in Table 1.

The essential features of the Langmuir adsorption isotherm parameter can be used to predict the affinity between the adsorbate and adsorbent using a dimensionless constant called separation factor or equilibrium parameter ( $R_L$ ), which is expressed by the following relationship (3) [35]:

$$R_L = \frac{1}{1 + bC_0} \quad (3)$$

where  $C_0$  is the initial dye concentration (mg/dm<sup>3</sup>) and  $b$  is the Langmuir equilibrium constant (dm<sup>3</sup>/mg). The value of  $R_L$  indicates the type of Langmuir

isotherm: irreversible ( $R_L = 0$ ), linear ( $R_L = 1$ ), unfavorable ( $R_L > 1$ ), or favorable ( $0 < R_L < 1$ ) [35]. The values of  $R_L$  calculated for different initial MY concentrations were found to be between 0.88 and 0.99, indicating that the adsorption of MY onto GMCNs is favorable.

The Freundlich equation characterized by the heterogeneity factor  $1/n$  is an empirical equation and it can be written as follows (4) [33,36]:

$$\log q_e = \log K_F + \frac{1}{n} \log C_e \quad (4)$$

where  $q_e$  is the solid-phase sorbate concentration in equilibrium (mg/g),  $C_e$  is the liquid-phase sorbate concentration in equilibrium (mg/dm<sup>3</sup>),  $K_F$  is the Freundlich constant (dm<sup>3</sup>/g), and  $1/n$  is the heterogeneity factor. “ $n$  value” indicates the degree of non-linearity between solution concentration and adsorption as follows: if  $n = 1$ , then adsorption is linear; if  $n < 1$ , then adsorption is a chemical process; and if  $n > 1$ , then adsorption is a physical process [37]. In the present study, since  $n$  was calculated as 4.47 (see Table 1), the adsorption of MY onto GMCNs is a physical process.

The correlation coefficients ( $R^2$ ) for the different models given in Table 1 suggest that the experimental data for MY adsorption onto GMCNs can be better

Table 2

Comparison of the linear first-order and second-order adsorption rate constants, calculated  $q_e$  and  $R^2$  values for different initial dye concentrations

Initial concentration (mM)	First-order kinetic model			Second-order kinetic model		
	$k_1$ ( $\text{h}^{-1}$ )	$q_e$ (mg/g)	$R^2$	$k_2$ (g/mg h)	$q_e$ (mg/g)	$R^2$
2.5	0.14	261	0.79	$3.6 \times 10^{-4}$	370	0.96
3.8	0.33	632	0.88	$1.03 \times 10^{-3}$	500	0.99
5.6	0.28	500	0.96	$1.07 \times 10^{-3}$	667	0.99

represented by the Langmuir equation compared to the Freundlich model. The value of  $q_m$  obtained from the Langmuir plots is mainly consistent with the experimental data, suggesting that the adsorption process is mainly monolayer.

### 3.4. Adsorption kinetics

In order to investigate the mechanism of adsorption, the pseudo-first-order and pseudo-second-order models were used to correlate the experimental data. The pseudo-first-order model of Lagergren (5) is given as [33,38]:

$$\log(q_e - q_t) = \log q_e - k_1 \frac{t}{2.303} \quad (5)$$

where  $q_e$  and  $q_t$  are the amounts of MY adsorbed onto GMCNs (mg/g) at equilibrium and at time  $t$ , respectively, and  $k_1$  is the rate constant of the first-order adsorption ( $\text{min}^{-1}$ ). The straight line plots of  $\log(q_e - q_t)$  against  $t$  were used to determine the rate constant,  $k_1$ , and correlation coefficients.

The pseudo-second-order model (6) can be expressed as [33,39]:

$$\frac{t}{q_t} = \frac{1}{k_2 q_e^2} + \frac{t}{q_e} \quad (6)$$

where  $k_2$  is the rate constant of the second-order adsorption ( $\text{mg/g min}^{-1}$ ). The straight line plots of  $t/q_t$  against  $t$  were used to determine the rate constant,  $k_2$ , and correlation coefficient [29]. It is more likely to predict behavior over the whole range of adsorption.

The first-order and second-order adsorption rate constants, calculated  $q_e$  and  $R^2$  values for different initial MY concentrations at 25°C and at pH 4, are given in Table 2. As shown in Table 2, the pseudo-second-order model is more suitable to represent the experimental data on the adsorption process.

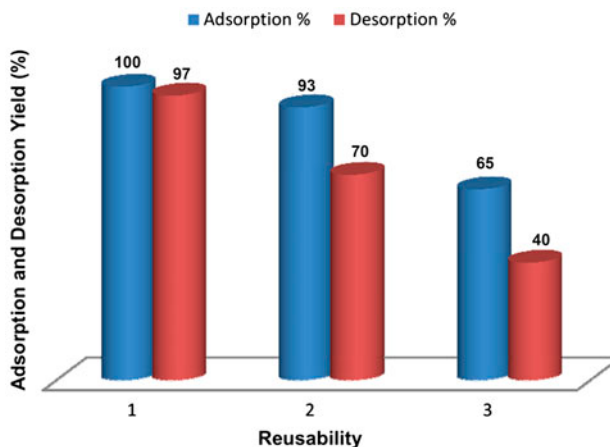


Fig. 8. Adsorption and desorption yield of MY onto GMCNs.

### 3.5. Reusability

Desorption studies as a function of pH were conducted to analyze the possibility of reusing the adsorbent for further adsorption and to make the process more economical. After adsorption experiments, the dye-loaded GMCNs were washed with distilled water to remove any non-adsorbed dye and then were incubated with  $\text{NH}_4\text{OH}/\text{NH}_4\text{Cl}$  buffer. To investigate the reusability of the adsorbent, for each period, GMCNs after desorption were separated with the help of a magnet and reused in adsorption experiments and the process was carried out three times (see Fig. 8). Desorption results for reusability were 97, 70, and 40%, respectively, for three repeats.

## 4. Conclusions

Thus, on the basis of the above-mentioned findings, it can be safely concluded that the dye MY can be easily removed by the adsorbent, GMCNs. The adsorption process is pH dependent and highest amounts of dye can be removed at pH 4.0. The maximum removal of MY is achieved at its 2.5-mM concentration using

70-mg GMCNs. It is also established that almost 17 h are sufficient to attain equilibrium in the present case and the adsorption follows pseudo-second-order rate expression. The values of thermodynamic parameters obtained for the adsorption process indicated that the Langmuir isotherm model agrees with experimental data better than the Freundlich. The values of separation factor ( $R_L$ ) calculated for different initial MY concentrations showed that the adsorption of MY onto GMCNs is favorable. Since  $n$  was calculated as 4.47 from the Freundlich equation (see Table 1), the adsorption of MY onto GMCNs is a physical process.

In addition, GMCNs can be regenerated efficiently using alkaline solution at pH 10.0; thus, the adsorbent was used for three repeated cycles for the dye removal. The technique used in this study offered a convenient and efficient method for the preparation of GMCNs, which facilitated a more efficient adsorption of dye from aqueous solution (adsorbed 65% of MY after three repeats) and avoided secondary pollution of the adsorbent to water.

### Acknowledgments

This project is funded by the financial support from Dicle University Research Fund (DUBAP, Project No. 13-ZEF-28, DUBAP, Project No. 13-ZEF-85).

### References

- [1] A. Mittal, V.K. Gupta, A. Malviya, J. Mittal, Process development for the batch and bulk removal and recovery of a hazardous, water-soluble azo dye (Metanil Yellow) by adsorption over waste materials (Bottom Ash and De-Oiled Soya), *J. Hazard. Mater.* 151 (2008) 821–832.
- [2] O. Anjaneya, S.Y. Souche, M. Santoshkumar, T.B. Karegoudar, Decolorization of sulfonated azo dye Metanil Yellow by newly isolated bacterial strains: *Bacillus* sp. strain AK1 and *Lysinibacillus* sp. strain AK2, *J. Hazard. Mater.* 190 (2011) 351–358.
- [3] G. Xiaoyao, W. Qin, D. Bin, Z. Yakun, X. Xiaodong, Y. Liangguo, Y. Haiqin, Removal of Metanil Yellow from water environment by amino functionalized graphenes (NH<sub>2</sub>-G)—Influence of surface chemistry of NH<sub>2</sub>-G, *Appl. Surf. Sci.* 284 (2013) 862–869.
- [4] T. Robinson, G. McMullan, R. Marchant, P. Nigam, Remediation of dyes in textile effluent: A critical review on current treatment technologies with a proposed alternative, *Bioresour. Technol.* 77 (2001) 247–255.
- [5] M. Naushad, A. Mittal, M. Rathore, V. Gupta, Ion-exchange kinetic studies for Cd(II), Co(II), Cu(II), and Pb(II) metal ions over a composite cation exchanger, *Desalin. Water Treat.* 54 (2015) 2883–2890.
- [6] J. Mittal, A. Mittal, in: Dr. S.K. Sharma, Hen. Feather, A remarkable adsorbent for dye removal, green chemistry for dyes removal from wastewater, Scrivener Publishing LLC, Beverly, 2015, pp. 409–857.
- [7] M.T. Sulak, H.C. Yatmaz, Removal of textile dyes from aqueous solutions with eco-friendly biosorbent, *Desalin. Water Treat.* 37 (2012) 169–177.
- [8] M. Vaez, A.Z. Moghaddam, N.M. Mahmoodi, S. Alijani, Decolorization and degradation of acid dye with immobilized titania nanoparticles, *Process Saf. Environ. Prot.* 90 (2012) 56–64.
- [9] İ. Özbay, U. Özdemir, B. Özbay, S. Veli, Kinetic, thermodynamic, and equilibrium studies for adsorption of azo reactive dye onto a novel waste adsorbent: Charcoal ash, *Desalin. Water Treat.* 51 (2013) 6091–6100.
- [10] M.C. Shih, Kinetics of the batch adsorption of methylene blue from aqueous solutions onto rice husk: Effect of acid-modified process and dye concentration, *Desalin. Water Treat.* 37 (2012) 200–214.
- [11] J. Mittal, V. Thakur, A. Mittal, Batch removal of hazardous azo dye Bismark Brown R using waste material hen feather, *Ecol. Eng.* 60 (2013) 249–253.
- [12] H. Daraei, A. Mittal, J. Mittal, H. Kamali, Optimization of Cr(VI) removal onto biosorbent eggshell membrane: Experimental & theoretical approaches, *Desalin. Water Treat.* 52 (2014) 1307–1315.
- [13] J. Mittal, D. Jhare, H. Vardhan, A. Mittal, Utilization of bottom ash as a low-cost sorbent for the removal and recovery of a toxic halogen containing dye eosin yellow, *Desalin. Water Treat.* 52 (2014) 4508–4519.
- [14] G. Sharma, M. Naushadb, D. Pathania, A. Mittal, G.E. El-Desoky, Modification of *Hibiscus cannabinus* fiber by graft copolymerization: Application for dye removal, *Desalin. Water Treat.* 54(2015) 3114–3121, doi: 10.1080/19443994.2014.904822.
- [15] A. Mittal, L. Kurup, Column operations for the removal and recovery of a hazardous dye 'acid red - 27' from aqueous solutions, using waste materials-bottom ash and de-oiled soya, *Ecol. Environ. Conserv.* 13 (2) (2006) 181–186.
- [16] R.N. Goyal, A. Kumar, A. Mittal, Oxidation chemistry of adenine and hydroxyadenines at pyrolytic graphite electrodes, *J. Chem. Soc., Perkin Trans. 2* (1991) 1369–1375.
- [17] H. Zhu, M. Zhang, Y. Liu, L. Zhang, R. Han, Study of congo red adsorption onto chitosan coated magnetic iron oxide in batch mode, *Desalin. Water Treat.* 37 (2012) 46–54.
- [18] W. Wu, Q. He, C. Jiang, Magnetic iron oxide nanoparticles: Synthesis and surface functionalization strategies, *Nanoscale Res. Lett.* 3 (2008) 397–415.
- [19] M.N.V. Ravi Kumar, A review of chitin and chitosan applications, *React. Funct. Polym.* 46 (2000) 1–27.
- [20] K.Z. Elwakeel, Removal of reactive black 5 from aqueous solutions using magnetic chitosan resins, *J. Hazard. Mater.* 167 (2009) 383–392.
- [21] W.S. Wan Ngah, L.C. Teong, M. Hanafiah, Adsorption of dyes and heavy metal ions by chitosan composites: A review, *Carbohydr. Polym.* 83 (2011) 1446–1456.
- [22] Z.G. Hu, J. Zhang, W.L. Chan, Y.S. Szeto, The sorption of acid dye onto chitosan nanoparticles, *Polymer* 47 (2006) 5838–5842.
- [23] W. Ngah, S. Ab Ghani, A. Kamari, Adsorption behaviour of Fe(II) and Fe(III) ions in aqueous solution on

- chitosan and cross-linked chitosan beads, *Bioresour. Technol.* 96 (2005) 443–450.
- [24] A. Kamari, W.S.W. Ngah, M.Y. Chong, M.L. Cheah, Sorption of acid dyes onto GLA and H<sub>2</sub>SO<sub>4</sub> cross-linked chitosan beads, *Desalination* 249 (2009) 1180–1189.
- [25] B. Tural, S. Tural, A.S. Demir, Carboligation reactions mediated by benzoylformate decarboxylase immobilized on a magnetic solid support, *Chirality* 25 (2013) 415–421.
- [26] S. Tural, B. Tural, M.S. Ece, E. Yetkin, N. Özkan, Kinetic approach for the purification of nucleotides with magnetic separation, *J. Sep. Sci.* 37 (2014) 3370–3376.
- [27] M.S. Chiou, G.S. Chuang, Competitive adsorption of dye metanil yellow and RB15 in acid solutions on chemically cross-linked chitosan beads, *Chemosphere* 62 (2006) 731–740.
- [28] A. Bousher, X. Shen, R.C.J. Edyvean, Removal of coloured organic matter by adsorption onto low-cost waste materials, *Water Res.* 31 (1997) 2084–2092.
- [29] G.Y. Li, Y.R. Jiang, K.L. Huang, P. Ding, J. Chen, Preparation and properties of magnetic Fe<sub>3</sub>O<sub>4</sub>-chitosan nanoparticles, *J. Alloys. Compd.* 466 (2008) 451–456.
- [30] G. Crini, P.M. Badot, Application of chitosan, a natural aminopolysaccharide, for dye removal from aqueous solutions by adsorption processes using batch studies: A review of recent literature, *Prog. Polym. Sci.* 33 (2008) 399–447.
- [31] A.H. Chen, S.M. Chen, Biosorption of azo dyes from aqueous solution by glutaraldehyde-crosslinked chitosans, *J. Hazard. Mater.* 172 (2009) 1111–1121.
- [32] I. Langmuir, The constitution and fundamental properties of solids and liquids. Part 1. solids, *J. Am. Chem. Soc.* 38 (1916) 2221–2295.
- [33] H. Daraei, A. Mittal, M. Noorisepehr, J. Mittal, Separation of chromium from water samples using eggshell powder as a low-cost sorbent: Kinetic and thermodynamic studies, *Desalin. Water Treat.* 53 (2015) 214–220.
- [34] D.M. Ruthven, Principles of adsorption and adsorption processes, John Wiley and Sons, New York, NY, 1984.
- [35] T.W. Weber and R.K. Chakravorti, Pore and solid diffusion models for fixed-bed adsorbers, *AIChE J.* 20 (1974) 228–238.
- [36] H.M.F. Freundlich, Over the adsorption in solution, *J. Phys. Chem.* 57 (1906) 385–471.
- [37] F. Haghseresht, G. Lu, Adsorption characteristics of phenolic compounds onto coal-reject-derived adsorbents, *Energy Fuels* 12 (1998) 1100–1107.
- [38] S. Lagergren, About the theory of so-called adsorption of soluble substance, *Kungliga Svenska Vetenskapsakademiens: Handlingar* 24 (1898) 1–39.
- [39] G. McKay, Y.S. Ho, Pseudo-second order model for sorption processes, *Process Biochem.* 34 (1999) 451–465.